Materials Today Communications 31 (2022) 103635

Contents lists available at ScienceDirect

Materials Today Communications

journal homepage: www.elsevier.com/locate/mtcomm

# Tuning of 2D cultured human fibroblast behavior using lumichrome photocrosslinked collagen hydrogels

Krister Gjestvang Grønlien [a,*], Mona Elisabeth Pedersen [b], Sissel Beate Rønning [b], Nina Therese Solberg [b], Hanne Hjorth Tønnesen [a]

[a] Section for Pharmaceutics and Social Pharmacy, Department of Pharmacy, University of Oslo, P.O. Box 1068 Blindern, NO-0316 Oslo, Norway
[b] Department of Raw Material and Process Optimization, Nofima AS, P.O. Box 210, NO-1431 Ås, Norway

ARTICLE INFO

*Keywords:*
Collagen
Lumichrome
Fibroblasts

ABSTRACT

Collagen is extensively used in fabrication of hydrogels for biomedical applications but needs improvement after its isolation from tissues due to slow gelation and poor mechanical properties. Crosslinking could tailor such properties. Collagen has previously been crosslinked by chemical or photochemical methods. Chemical crosslinkers are often toxic, and the crosslinking reaction is difficult to control. Photochemical crosslinkers are usually biocompatible compounds that are activated upon irradiation. Riboflavin (vitamin $B_2$), a photochemical crosslinker of collagen, photodegrades to lumichrome upon irradiation. Cyclodextrins have previously been used to increase the aqueous solubility of lumichrome and regulate collagen self-assembly. In this study, lumichrome dissolved by cyclodextrin complexation was used as a photochemical crosslinker of collagen. Lumichrome photocrosslinking reduced the gelation time to 10 s, compared to 90 min for physical crosslinking. The formed hydrogels exhibited increased elasticity, water absorption properties and water holding capacity compared to physically crosslinked collagen hydrogels and riboflavin photocrosslinked collagen hydrogels. Fibroblasts achieved a myofibroblastic phenotype when cultivated in 2D on lumichrome photocrosslinked gels as observed from histology. These biocompatible photocrosslinked hydrogels could have potential applications in biomedical applications, such as wound healing.

## 1. Introduction

Collagen is a structural protein that is considered as a good material candidate for fabrication of biocompatible and biodegradable scaffolds. Collagen is composed of three α-chains forming the characteristic triple helix structure of the protein. The α-chains consists of repeating triplets of the amino acids Glycine-X-Y, where X and Y are often proline and its metabolite hydroxyproline [1]. As the main structural protein in the extracellular matrix and connective tissue, collagen serves important functions in the body as support for cell growth and migration in various biological processes [2].

The production of scaffolds suitable for cell growth can be used in tissue engineering techniques. These techniques are considered as emerging technologies for production and engineering of tissue and biomimicking constructs and organs [3–5]. In tissue engineering, scaffolds are fabricated to serve as synthetic extracellular matrices to organize cells into three dimensional architectures, providing mechanical support and allowing for optimal growth, nutrition and biological signaling [6,7]. Examples of scaffold fabrication techniques are electrospinning, bioprinting, production of hybrid scaffolds and hydrogels [8]. Collagen is extensively used in such applications. The use has been considered somewhat limited due to low viscosity, slow gelation and poor mechanical properties of fabricated constructs. Previous attempts to overcome these challenges include increasing collagen concentration, using protein or polymer blends, forming the structures directly into a supportive gelatin slurry bath (commonly known as FRESH bioprinting) or chemically modifying the collagen with methacrylate [9–13]. Recently, the effects of riboflavin (Vitamin $B_2$, RF) photocrosslinking on the printability of collagen bioinks for bioprinting have been studied. Diamantides *et al.* (2017) reported that blue light-activated RF crosslinking improved the viscoelastic properties and printability of the bioink [14]. The study found that the RF photocrosslinking increased the storage modulus even before the bioink was brought to 37 °C, which is normally necessary for collagen to physically

* Corresponding author.
*E-mail address:* k.g.gronlien@farmasi.uio.no (K.G. Grønlien).

https://doi.org/10.1016/j.mtcomm.2022.103635
Received 18 May 2021; Received in revised form 11 March 2022; Accepted 29 April 2022
Available online 5 May 2022

crosslink. RF photocrosslinking of collagen is commonly used in corneal crosslinking (CXL) for the treatment of the eye disease keratoconus [15]. Irradiation of RF results in photodegradation to lumichrome (LC) and lumiflavin (LF) in acidic and neutral, and alkaline solutions, respectively [16,17]. Both LC and LF are considered as more photostable than RF and are efficient photogenerators of singlet oxygen in aqueous media [17,18]. LC has previously been investigated as a potential photosensitizer for inactivation of pathogens by antimicrobial photodynamic therapy (aPDT). The photosensitizer absorbs in both UVA and the blue region of the electromagnetic spectrum. The use of these metabolites as photosensitizers are, however, limited due to their low aqueous solubility [18].

Cyclodextrins (CDs) have been used to increase the water solubility of LC by a tenfold [18]. This increases the potential for LC as a photosensitizer. CDs are cyclic oligosaccharides with a hydrophobic inner and a hydrophilic outer structure [19]. They are stable in bases and weak organic acids but may be hydrolyzed in strong acids [20,21]. Collagen has previously been modulated with CDs in order to regulate the collagen self-assembly and producing materials similar to native cornea [22]. CDs will bind to aromatic residues on the collagen molecule resulting in increased viscosity through collagen self-assembly [22]. CDs have as well been incorporated into collagen scaffolds to promote binding of growth factors and modulate stem cell activity and to control the delivery of active pharmaceutical ingredients [23,24].

Collagen is a protein interesting for tissue engineering applications, including the treatment of dermal loss and wound healing, mimicking the native structure of the skin. During wound healing, collagen is degraded by proteolytic enzymes to peptides, which are chemotactic to cells involved in the remodeling of the skin [25,26]. The invasion of cells, among other fibroblasts, is important for migration and proliferation into the wound site and synthesis of extracellular macromolecules. In granulation tissue, the fibroblasts are activated further into myofibroblasts, expressing α-smooth muscle actin (α-SMA). Myofibroblasts are involved in the wound healing by production and organization of the extracellular matrix [27]. It is further involved in wound contraction and scarring [28]. In all steps of the wound healing process, proteolytic enzymes play a major role modifying the wound matrix allowing cell migration and remodeling of the skin. These include matrix metalloproteinases (MMPs) and tissue inhibitors of MMPs (TIMPs). MMPs are important for collagen in wound healing, digesting the collagen to fragments, that may work chemotactically to cells involved in the healing process [29]. Syndecan-4 (SDC-4) is a cell receptor protein, which is a target for MMP-2 activity. Its extracellular domain is cleaved by this protease among others, thereby fine tuning the biological activity of the receptor protein [30]. SDC-4 is a prominent regulator of focal adhesion and actin-cytoskeletal organization formation in fibroblasts, and therefore a regulator of fibroblast cell adhesion and migration [31–33]. This makes SDC-4 important for the wound healing process [34].

In the present study, the aim was to investigate the effects of CD modulation and LC photocrosslinking on collagen hydrogels. Collagen was isolated in-house using turkey (*Meleagris gallopavo*) byproducts, as this sustainable material from Norwegian industrially produced poultry meat is shown to have several beneficial properties compared with collagen from mammalian and aquatic species. We have previously shown that this material, containing high purity collagen type I and III, retained the native triple helix structure also after isolation. Further, the material has a high thermal stability and is cytocompatible, making it suitable for pharmaceutical and biomedical purposes [35]. The physical properties of the hydrogels were studied with respect to crosslinking density, water retention, mechanical properties, thermal properties and enzyme mediated scaffold degradation. Cell studies were conducted with fibroblasts seeded on top of the hydrogels. Cell morphology, cell viability, enzyme expression and secretion of proteins involved in extracellular matrix production and differentiation were monitored, as well as expression of corresponding genes. To our knowledge, this is the first paper describing the use of LC as a photochemical crosslinker for collagen.

## 2. Materials and methods

All experiments were performed at 25 °C unless other stated. LC photocrosslinked collagen hydrogels were crosslinked at 4 °C and used directly, or further physically crosslinked at 37 °C. Physically crosslinked collagen hydrogels, RF photocrosslinked collagen hydrogels and CD modulated collagen hydrogels were crosslinked at 37 °C.

### 2.1. Raw materials, chemicals, and reagents

Collagen isolated from industrially produced turkey (*Meleagris gallopavo*) rest raw materials was prepared as described in Grønlien *et al.* 2019 [35]. In brief, turkey tendons were manually cleaned and freeze dried for 48 h. A 0.5 M acetic acid solution with pepsin (1:10) was added to enzymatically hydrolyze the material. The hydrolyzed material was centrifuged, and the supernatant was collected. The collagen was precipitated by the addition of 4 M NaCl (1:3) and centrifuged. The collagen was re-solubilized in 0.5 M acetic acid and dialyzed against distilled water for 3 days. The dialyzed solution was further freeze dried to obtain dry collagen. Other reagents were of analytical grade and were purchased from Merck KGaA (Darmstadt, Germany). Cell medium and components were all purchased from Thermo Fischer Scientific (Waltham, MA, USA).

### 2.2. Preparation of collagen hydrogels

The preparation of collagen hydrogels by physical crosslinking, LC photocrosslinking, RF photocrosslinking and CD modulation is described below. The preparation parameters are summarized in Table 1.

#### 2.2.1. Hydrogels prepared by lumichrome photocrosslinking (LC gels)

LC photocrosslinked hydrogels (LC gels) were prepared by a direct photocrosslinking method. (2-Hydroxypropyl)-β-cyclodextrin (HPβCD) was dissolved in 20 mM acetic acid to a final concentration of 5% (w/v). LC was dissolved in the acidic HPβCD-solution to a final concentration of 250 μM. Collagen was dissolved in the acidic HPβCD-solution over 24 h to a final concentration of 5 mg/ml. The collagen solution was neutralized to pH 7.4 by the addition of 10X phosphate buffered saline (PBS) (0.1 × final volume of the combined solution), 1 M NaOH (0.023 × volume of added collagen-HPβCD solution) and Milli-Q water to give a final concentration of 4 mg/ml collagen, 200 μM LC and 1X PBS. The neutralized solutions were crosslinked by irradiation with either UVA ($\lambda_{max}$ = 365 nm, 16.0 mW/cm$^2$) or blue light ($\lambda_{max}$ = 405 nm, 17.8 mW/cm$^2$) (Bio X, Cellink, Gothenburg, Sweden) for 10 s. The gels were incubated at 37 °C for 90 min to complete the crosslinking procedure.

To distinguish the effects of LC and HPβCD in cell studies, CD modulated collagen hydrogels (CD gels) were prepared with 5% (w/v) HPβCD added to 20 mM acetic acid without the addition of LC and photocrosslinking as a control.

#### 2.2.2. Hydrogels prepared by physical crosslinking (Col gels)

Physically crosslinked hydrogels (Col gels) were included as controls without photocrosslinking and prepared by a direct gelation method. Collagen was dissolved in 20 mM acetic acid over 24 h to a concentration of 5 mg/ml. The collagen solution was neutralized to pH 7.4 by the addition of 10X PBS (0.1 × final volume of the combined solution) and 1 M NaOH (0.023 × volume of added collagen solution) and diluted with Milli-Q water to give a final concentration of 4 mg/ml collagen and 1X PBS. The neutralized solution was incubated in the dark at 37 °C for 90 min to initiate gelling and self-assembly of the collagen.

**Table 1**
Summary of preparation parameters of collagen hydrogels.

| Gel sample | Final collagen concentration | Final cyclodextrin concentration | Final photocrosslinker concentration | Final pH | Incubation | Irradiation parameters | Post-irradiation incubation |
|---|---|---|---|---|---|---|---|
| *Col gels* | 4 mg/ml | N. A. | N. A. | 7.4 | 37 °C, 90 min | N. A. | N. A. |
| *LC gels* | 4 mg/ml | 4% | 200 μM LC | 7.4 | N. A. | 10 s, $\lambda_{max}$ = 405 nm | 37 °C, 90 min |
| *RF gels* | 4 mg/ml | N. A. | 265 μM RF | 7.4 | 37 °C, 60 min | 4 min, $\lambda_{max}$ = 365 nm | 37 °C, 30 min |
| *CD gels* | 4 mg/ml | 4% | N. A. | 7.4 | 37 °C, 90 min | N. A. | N. A. |

#### 2.2.3. Hydrogels prepared by riboflavin photocrosslinking (RF gels)

RF photocrosslinked hydrogels (RF gels) were included as a literature-described photocrosslinked hydrogel control and prepared by a two-step gelation and photocrosslinking method. The hydrogels were prepared as for the Col gels, except with the addition of riboflavin 5′-monophosphate sodium salt to a final concentration of 0.01% (w/v) (265 μM). The neutralized solution was incubated in the dark at 37 °C for 1 h to initiate gelling and self-assembly of the collagen. The collagen hydrogels were irradiated with UVA ($\lambda_{max}$ = 365 nm, 2.94 mW/cm$^2$) (Polylux-PT, Dreve, Germany), for 4 min to form interhelical crosslinks. The crosslinking procedure was then completed by incubating the hydrogels in the dark at 37 °C for 30 min

#### 2.2.4. Freeze-drying of hydrogels

Collagen hydrogels were freeze-dried prior to some analysis to avoid influence from water. The gels were frozen at − 80 °C for 1 h prior to freeze drying at 0.011 mbar for 24 h, including 1 h final drying at 0.0010 mbar (Alpha 2–4 LD Plus Freeze Dryer, Martin Christ, Germany) resulting in dry constructs.

### 2.3. Physical characterization of hydrogels

#### 2.3.1. Viscosity measurements

Viscosity measurements were performed on a Brookfield DV2T viscometer (Brookfield Engineering Laboratories, Inc., Middleboro, MA, USA) with spindles CPA-40Z (low viscosity samples < 10 mPa s; accuracy: ± 0.1 mPa·s; sample volume: 0.5 ml) and CPA-52Z (medium viscosity samples 10 – 300 mPa·s; accuracy: ± 3.1 mPa·s and high viscosity samples ≥ 1500 mPa·s; accuracy: ± 31.0 mPa·s; sample volume: 0.5 ml). The temperature was kept constant at 25 °C during the viscosity measurements (Grant LTD6G water bath, Grant Instruments, Cambridge, Ltd., Royston, UK). An average measurement was performed with the end condition parameter fixed at 2 min and speed depending on the expected viscosity (30 rpm for samples ≤ 300 mPa·s, 5 rpm for samples 300 – 1500 mPa·s, and 3 rpm for samples ≥ 1500 mPa·s).

#### 2.3.2. Swelling ratio (SR)

Freeze-dried collagen hydrogels were soaked in PBS at room temperature overnight. The rehydrated hydrogels were then removed from the solution, gently dabbed with an absorbent paper to remove excess fluid and weighed. The hydrogels contain water soluble compounds which will diffuse out in the media after rehydration and induce a weight-loss. The rehydrated hydrogels were therefore freeze-dried according to Section 2.2.4 and weighed dry. The Swelling Ratio (SR) for each sample was calculated using Eq. (1).

$$SR(\%) = \frac{W_{wet} - W_{dry}}{W_{dry}} \times 100\%, \quad (1)$$

where $W_{wet}$ is the weight of the samples soaked for overnight in PBS and $W_{dry}$ is the weight of the samples that were freeze-dried after rehydration.

#### 2.3.3. Water holding capacity (centrifugal dehydration)

Col, RF, LC and CD gels were compared according to their water holding capacity. The hydrogels were placed in a Corning™ Costar™ Spin-X™ Centrifuge Tube Filter (Corning Inc. Life Sciences, Corning, NY, USA) with 0.45 μm pores and centrifuged at 2000 rpm (394*g*) [36]. The water retention at fixed time points between 2 and 240 min were calculated based on the weight ratio after and before centrifugation ($W/W_0$). The water holding capacity was defined as the percentage of weight remaining after centrifugation for 240 min

#### 2.3.4. Enzyme-mediated scaffold degradation

Enzyme-mediated scaffold degradation was studied by collagenase digestion of the prepared hydrogels. Type I collagenase from *Clostridium histolyticum* (C0130, Sigma-Aldrich, Saint Louis, MO, USA) was dissolved in Dulbecco's Phosphate Buffered Saline (DPBS) with 100 mg/l $MgCl_2$ and 100 mg/l $CaCl_2$ (Gibco, Life Technologies Corp., Grand Island, NY, USA) to a concentration of 5 CDU/ml. Hydrogels prepared were equilibrated in DPBS for 30 min. Further, the hydrogels were treated with the collagenase solution and incubated at 37 °C at 100 rpm in an orbital shaker (ES-20, Biosan Ltd., Latvia). Remaining hydrogels were removed from the solution, gently dabbed with an absorbent paper, weighed, and compared with untreated hydrogels at fixed time points between 2 and 24 h. The collagenase solution was changed at every 3rd sampling.

#### 2.3.5. Mechanical properties (macroindentation)

Mechanical properties of the prepared hydrogels were studied using TA-XTplusC Texture Analyser (Stable Micro Systems, Godalming, UK) in compression mode. The hydrogels were prepared in 24-well plates (VWR International., Radnor, PA, USA) according to the described preparation procedures. The resulting cylindrical gels equilibrated in PBS overnight (4 °C) and exposed to constant pressure at 0.1 mm/s with a maximum strain set to 60% by a cylindrical flat-ended indenter (ø = 6 mm) attached to a 500 g load cell. The probe was positioned approximately 2 mm above the sample prior to analysis. The stress (kPa) was calculated by the force and load-bearing area (A) of the gels and plotted against the strain. The elastic moduli ($E$) were calculated using Eq. (2).

$$E = \frac{(1 - \nu^2)\, F_c}{2\partial r}, \quad (2)$$

where $\nu$ is the Poisson's ratio, $F_c$ is the applied force (N), $\delta$ is the indentation depth and $r$ is the indenter radius [37]. Poisson's ratio was estimated to 0.5 for the hydrogels.

#### 2.3.6. Thermal analysis

Differential scanning calorimetry (DSC) experiments were performed on freeze-dried collagen hydrogels using a DSC822$^e$ Differential Scanning Calorimeter (Mettler Toledo Intl. Inc., Greifensee, Switzerland). DSC thermograms were recorded for samples containing 0.9–1.1 mg collagen at a constant heating rate of 10 °C/min in the temperature range 20–140 °C and under dry nitrogen purge (80 ml/min). The samples were placed in aluminum sample pans with pierced lids. An empty

pan was used as reference. The transition temperature of collagen in the hydrogels was defined at the minimum of the transition peak when integrated.

#### 2.3.7. 2,4,6-trinitrobenzenesulfonic acid (TNBS) assay

The content of primary amine groups in freeze-dried collagen hydrogels was determined using a 2,4,6-trinitrobenzenesulfonic acid (TNBS) assay according to protocols described in the literature [38]. The TNBS assay is one of several methods used to measure the content of primary amines to decide the degree of hydrolysis or the reduction of primary amines due to crosslinking reactions where primary amines are the targets [39]. The whole samples containing 2 mg collagen were hydrated with 0.5 ml of 4% (w/v) $NaHCO_3$ overnight in the refrigerator. After complete hydration, 0.5 ml of a freshly prepared 0.05% (w/v) TNBS solution was added. The samples were incubated at 37 °C for 2 h before addition of 1.5 ml 6 M HCl. The samples were incubated at 60 °C for 90 min to dissolve any sample residuals. The samples were cooled down to room temperature and the absorbance at 320 nm was detected using a Synergy H1 Hybrid Multi-Mode Microplate Reader (Biotek, Bad Friedrichshall, Germany). All samples were measured against a blank prepared as described above except for the addition of 6 M HCl prior to adding TNBS. A calibration curve was prepared from a 5 mg/ml glycine stock solution diluted in 4% (w/v) $NaHCO_3$ and treated in the same way as the samples. The content of primary amines per 1000 amino acid residues (n/1000) was calculated from the standard curve with the assumption of collagen having an average molecular weight of amino acids of 90.1 g/mol [40].

#### 2.3.8. Scanning electron microscopy (SEM)

Scanning Electron Microscopy (SEM) was performed on the hydrogels after complete crosslinking procedure to assess the microstructure. Samples were fixed in 2% glutaraldehyde and 4% paraformaldehyde in PHEM buffer pH 7.4. After fixation, samples were washed 3 times for 15 min in PHEM buffer and subsequently dehydrated in a series of EtOH (50% up to 100%) followed by critical point drying (BAL-TEC CPD 030 Critical Point Dryer, BAL-TEC AG, Liechtenstein). Finally, samples were sputter coated with 10 nm platinum using a Cressington 308R Coating System (Ted Pella Incorporated, Redding, CA, USA), and analyzed using a Hitachi S-4800 Field Emission Scanning Electron Microscope (Hitachi, Tokyo, Japan).

#### 2.3.9. Peroxide content

The content of peroxides (mg/l $H_2O_2$) in the hydrogels after complete crosslinking procedure was measured using the Reflectoquant® test with corresponding test strips and RQflex® 10 instrument (Merck KGaA, Darmstadt, Germany) following the manufacturer's instructions. The hydrogels were transferred to Eppendorf tubes and vortexed for 10 s. The test strips were immersed in the liquid from the gels. The method is based on the transfer of peroxide oxygen to an organic redox indicator by peroxidases producing a blue oxidation product determined reflectometrically.

### 2.4. Cell studies

The cell studies consisted of three independent biological experiments, each performed in triplicates.

#### 2.4.1. Cell culture

Human primary dermal fibroblasts (ATCC, Manassas, VA, USA) were cultured in Dulbecco's modified Eagle's medium (DMEM) supplemented with 10% (v/v) fetal bovine serum (FBS), 100 U/ml penicillin, 100 μg/ml streptomycin and 250 μg/ml fungizone in tissue culture flasks. The cells were maintained at 37 °C in a humidified atmosphere of 5% $CO_2$. The cells were routinely sub-cultivated twice a week. The cells were examined by a Leica DM IL LED light microscope (Leica Microsystems Nussloch GmbH, Nußloch, Germany) during incubation. Cells between passages 3–10 were used in these experiments.

#### 2.4.2. Cell behavior on hydrogels

Evaluation of the suitability of the hydrogels as cell matrices was conducted for 48 h on proliferating cells. The different hydrogels (prepared as described above) were prepared in the wells of 24-well plates with glass bottom (MatTek Corp., Ashland, MA, USA). Fibroblasts were seeded on top of the hydrogels at a concentration of 50 000 cells/well. To monitor cell nuclei and dead cells, the cells were stained with NucBlue™ Live ReadyProbes™ (Hoechst 33342, bisbenzimide) and Propidium Iodide ReadyProbes™ (Life Technologies Corp., Eugene, OR, US), respectively. The dyes were used according to the manufacturer's instructions. Media was replaced prior to staining. The cells were examined and imaged with a Zeiss Axio Observer Z1 microscope and the ZEN 2.6 blue edition microscopy software suite (Zeiss, Jena, Germany). If necessary, the brightness and contrast of the image were manually adjusted across the entire image using Adobe Photoshop Elements 11.

#### 2.4.3. Immunofluorescence

Hydrogels (prepared as previously described) were prepared on the glass bottom of uncoated 35 mm petri dishes with the area of the glass bottom corresponding to the size of the wells of a 24-well plate (MatTek Corp., Ashland, MA, USA). Fibroblasts were seeded on top of the hydrogels at a concentration of 50 000 cells/well. After 48 h, the cells were washed twice with PBS and fixed with 4% (v/v) formaldehyde solution (252549, Sigma-Aldrich, Saint Louis, MO, USA) for 15 min. The cells were washed three times with 0.1% (v/v) Tween 20 in PBS (PBS-t) before permeabilizing with 0.1% (v/v) Triton X-100 in PBS for 10 min. After washing with PBS-t, the cells were blocked for 1 h (25 °C) or overnight (4 °C) using blocking buffer (ab126587, Abcam, Cambridge, UK) diluted in PBS-t before incubation with the primary antibody (Anti-alpha smooth muscle Actin antibody, ab5694, Abcam, Cambridge, UK) for 1 h (25 °C). Subsequent incubation with secondary antibody (Goat anti-Rabbit IgG (H+L) Cross-Adsorbed Secondary Antibody, Alexa Fluor™ 546, A-11010) for 1 h was performed after washing three times with PBS-t for 10 min. The cells were washed again thrice for 10 min before mounting the gels with Dako Fluorescence Mounting Medium (Dako North America, Carpinteria, CA, USA). For staining of the F-actin filaments, Alexa Fluor™ Phalloidin 488 (A12379, Life Technologies Corp., Eugene, OR, US, 1:200 dilution) was added together with the secondary antibody. Hoechst (1:1000 dilution, Invitrogen, Carlsbad, CA, USA) was used to counterstain cell nuclei. The cells were examined and imaged with a Zeiss Axio Observer Z1 microscope and the ZEN microscopy software suite (Zeiss, Jena, Germany). If necessary, the brightness and contrast of the image were manually adjusted across the entire image using Adobe Photoshop Elements 11.

#### 2.4.4. Sandwich enzyme-linked immunosorbent assays (ELISAs)

The protein secretion of matrix metalloproteinase-2 (MMP-2), tissue inhibitor of metalloproteinase-2 (TIMP-2) and shed syndecan-4 (SDC-4) was measured in the cell media supernatants. Fibroblasts were cultured on hydrogels in 24-well plates (VWR, Radnor, PA, USA) for 48 h at a concentration of 50 000 cells/well. The protein secretion was measured with commercial sandwich ELISA Kits (KHC3081 and EHTIMP2, Thermo Fisher Scientific, Inc., Waltham, MA, USA and ab213830, Abcam, Cambridge, UK). The ELISA kits were used according to the manufacturer's instructions. The optical density was detected using a Synergy H1 Hybrid Multi-Mode Microplate Reader (Biotek, Bad Friedrichshall, Germany).

#### 2.4.5. RNA extraction and reverse transcriptase quantitative polymerase chain reaction (RT-qPCR)

After sampling the supernatant for the Sandwich ELISA, the remaining gels were washed two times with PBS and preserved at − 80 °C for RT-qPCR experiments. The cells within the hydrogels were lysed and homogenized with a Precellys Evolution (Bertin Technologies

SAS, Montigny-le-Bretonneux, France) for 2 cycles of 30 s in RLT-lysis buffer (RNeasy® Plus Micro Kit, Qiagen, Hilden, Germany). The RNA was further purified using the RNeasy® Plus Micro Kit according to the manufacturer's protocol. cDNA was generated from the entire mRNA sample using TaqMan® Reverse Transcription Reagents (Applied Biosystem, Life Technologies, Carlsbad, CA, USA) according to the manufacturer's protocol. The cDNA (40 µl) was diluted to 65 µl with RNase-free water before aliquots were subjected to real-time qPCR by QuantStudio 5 Real-Time PCR System (Applied Biosystem, Life Technologies, Carlsbad, CA, USA). Amplification of cDNA by 45 two-step cycles (15 s at 95 °C for denaturation of DNA, 1 min at 60 °C for primer annealing and extension) was performed, and cycle threshold (Ct) values were obtained graphically (QuantStudio 5, Applied Biosystem, Design and Analysis Software version 1.5.1). The TaqMan® Gene Expression Assays used in this study are listed in Table 2. Gene expression of the samples was normalized against the average value of the housekeeping gene *EEF1A1*, and the ΔCt values were calculated according to the MIQE guidelines [41]. Comparison of the relative gene expression (fold change) of the fibroblasts between Col gels, LC gels and CD gels was derived by using the comparative Ct method. In short, values were generated by subtracting ΔCt values between two samples which gave a ΔΔCt value. The relative gene expression (fold change) was then calculated by the formula $2^{-\Delta\Delta Ct}$ [42]. The ΔΔCt value of LC gels and CD gels were calculated based on the mean ΔCt value of Col gels. The real-time qPCR was performed with three technical replicates in three independent cell culture experiments seeded out in triplicates.

### 2.5. Statistical analysis

The data was presented as mean ± standard deviation from three independent experiments. D'Agostino & Pearson tests were performed to determine the normality of the data. Statistical analyses were performed by one-way ANOVA with Tukey's multiple comparisons for normally distributed samples and Kruskal-Wallis test with Dunn's multiple comparison for samples not following a normal distribution. All statistics were performed using GraphPad Prism version 8.0.1 for Windows (GraphPad Software, La Jolla, CA, USA, www.graphpad.com). Differences were considered significant at $P < 0.05$.

### 2.6. Graphics

Illustrations were prepared in Microsoft PowerPoint. Graphs were created with GraphPad Prism version 8.0.1 for Windows (GraphPad Software, La Jolla, CA, USA, www.graphpad.com). Microscopy images were modulated with Adobe Illustrator CS6.

## 3. Results

### 3.1. Physical properties of collagen hydrogels are dependent on the preparation method and the crosslinking procedures

LC gels were formed directly after photocrosslinking of the neutralized collagen solution. A simplified illustration of the photocrosslinking by LC is illustrated in Fig. 1. To evaluate the optimal irradiation source for LC gels, the viscosity of gels before and directly after irradiation was measured. Collagen solutions with 5% (w/v) HPβCD and 250 µM LC exhibited a viscosity of 29.15 ± 0.44 mPa·s after neutralization, before crosslinking and 998.6 ± 55.2 mPa·s after irradiation by UVA (10 s, $\lambda_{max}$ = 365 nm), while exposing the solution to blue light (10 s, $\lambda_{max}$ = 405 nm) increased the viscosity to 1818 ± 83.8 mPa·s. Due to a superior viscosity and low deviation compared to the other formulations, we decided to continue with the formulation irradiated by blue light for 10 s. The Col gels, CD gels and RF gels appeared translucent, while LC gels appeared slightly yellow and transparent (Fig. 2). The primary amine content of Col gels was 12.99 ± 0.33/1000 amino acids and they had a swelling ratio of 2692 ± 437% and a low water retention (2.67 ± 0.53%). LC photocrosslinking of collagen resulted in gels with a significantly lower content of primary amines than Col and CD gels (10.66 ± 0.54/1000 amino acids), which is an indication of a higher crosslinking of the structure. The gels had a high swelling ratio (4214 ± 62%) and a high water retention (44.97 ± 3.04%). RF photocrosslinking of collagen resulted in gels with a low swelling ability (1487 ± 197%) and water retention (2.57 ± 0.06%). The content of primary amines was 12.24 ± 0.95/1000 amino acids. CD gels had a high primary amine content (15.63 ± 1.09/1000 amino acids), low water retention (5.12 ± 2.80%), but a high swelling ratio (4072 ± 140%) (Fig. 3a-c).

Exposing the gels to collagenase resulted in complete degradation within 24 h for all the gels, except RF gels. The weight of the LC gels became significantly reduced compared to the weight of the RF gels already after 3 h (Fig. 3d). After 24 h, 18.5 ± 1.9% of the RF gels were still intact (data not shown). Thermostability studies revealed the shrinkage temperature (loss of triple helical structure) for collagen in freeze-dried hydrogels. Col gels had a shrinkage temperature at 77.02 ± 2.19 °C, while photocrosslinking with RF slightly decreased the transition (not significantly) to 74.05 ± 3.20 °C. LC gels had a transition at 99.78 ± 1.81 °C, while CD gels had a transition at 98.10 ± 3.18 °C (Fig. 3e).

Compression tests illustrated the difference in the mechanical properties for the gels. Values for Young's moduli, ultimate compressive strengths and fracture points are presented in Table 3. Stress-strain curves are presented in Fig. 3f.

The collagen microstructure was studied by SEM. The structure of the hydrogels differed clearly by the presence of fibrillar structures in Col gels, CD gels and RF gels. The LC gels did not possess such higher order structures but presented a dense collagen network (Fig. 4a-d).

### 3.2. Fibroblasts seeded in 2D on LC gels exhibited a myofibroblastic phenotype and SDC-4 shedding together with a tendency of increased MMP-2/TIMP-2 ratio expression

Light microscopy investigation of the fibroblasts cultured on the different hydrogels showed different cell behavior dependent on type of crosslinking. Fibroblasts seeded on Col gels and CD gels were evenly distributed throughout the hydrogel surface (Fig. 5a left and right), however no cell clustering was observed, despite cell contact. Cells seeded on hydrogels with LC photocrosslinking, on the other hand, were self-organized into cell clusters and the fibroblasts had a more elongated morphology (Fig. 5a, middle). The cell viability was high, demonstrated by the low appearance of dead cells on either of the hydrogels (Fig. 5b). Cells seeded on top of hydrogels photocrosslinked using RF did, however, lead to dramatically reduced cell viability and were therefor not included in the following cell behavior experiments (Fig. S1). Quantification of the peroxide content of the hydrogels, which may be related to potential cell toxicity, revealed a content of 5.95 ± 0.21 mg $H_2O_2$/l for RF gels, while the other gels had a content under the quantification limit (< 0.2 mg $H_2O_2$/l).

When examining filamentous actin (F-actin) we clearly observed more prominent intracellular stress fibers in the Col and CD gels, while cells seeded onto LC gels demonstrated stronger staining of peripheral stress fibers (Fig. 6a). All the hydrogels seemed to stimulate the expression of the common myofibroblast marker α-SMA (Fig. 6b and c), however, cells seeded onto the LC hydrogel displayed a more mature

**Table 2**
List of TaqMan Gene Expression Assay probes used in RT-qPCR experiments.

| Gene | TaqMan Description | TaqMan assay ID |
|---|---|---|
| *EEF1A1* | Eukaryotic translation elongation factor 1 alpha 1 | Hs00265885_g1 |
| *ACTA2* | Actin, alpha 2, smooth muscle, aorta | Hs00909449_m1 |
| *SDC4* | Syndecan 4 | Hs00161617_m1 |
| *COL1A2* | Collagen type I alpha 2 chain | Hs01028939_g1 |

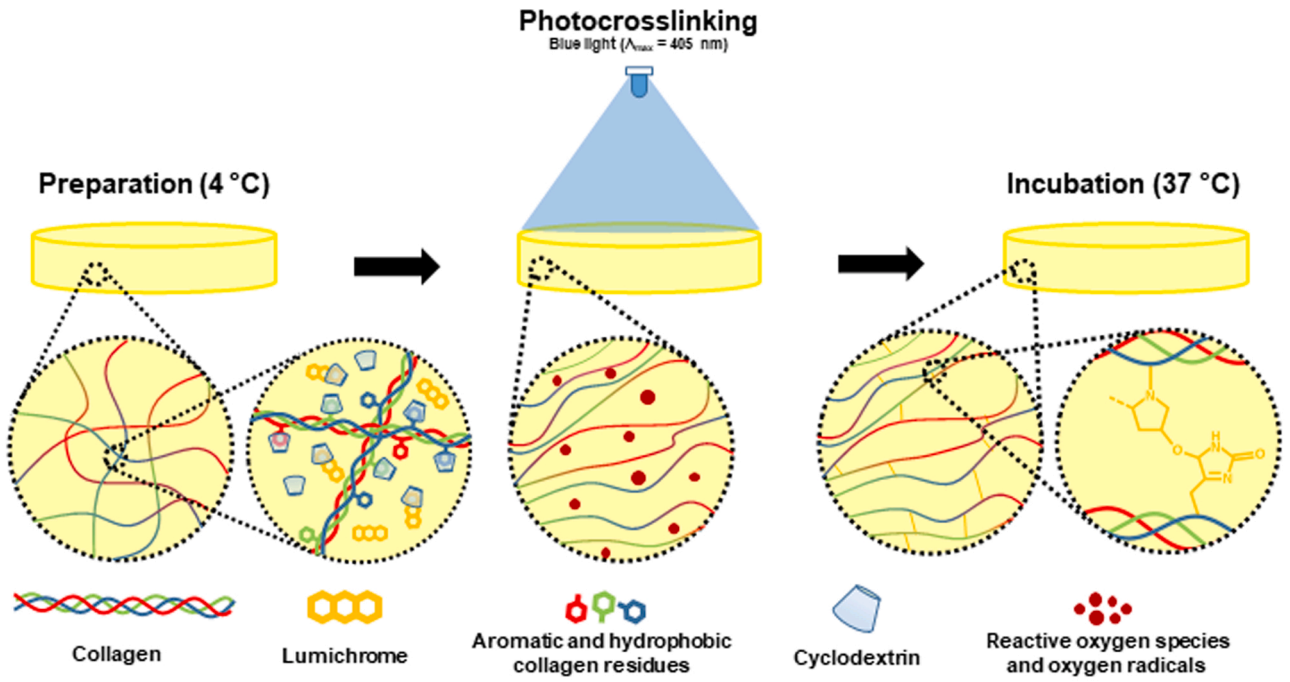


**Fig. 1.** Schematic illustration of LC photocrosslinking showing organization and crosslinking of collagen following irradiation. LC is complexed by CDs, which also can bind to aromatic and hydrophobic residues of collagen amino acids. Neutralization and irradiation of the solutions produce reactive oxygen species (ROS) and singlet oxygen ($^1O_2$). The ROS and $^1O_2$ react with reactive carbonyl groups in collagen amino acids, such as histidine (shown on schematic), which after interaction with reactive nucleophiles (e.g., hydroxyl on hydroxyproline, as shown, or primary amines on hydroxylysine) can generate inter- and intramolecular crosslinks between the collagen molecules [46,77]. This will increase strength and robustness of collagen gels formed.

**Fig. 2.** Appearance of the hydrogels depending on crosslinking procedure. From left: Col gel with translucent appearance, LC gel with slightly yellow and transparent appearance, CD gel with translucent appearance, and RF gel with yellow and translucent appearance. Gel edges are highlighted using dashed lines and the transparency is illustrated by a red logo in the background. (For interpretation of the references to color in this figure legend, the reader is referred to the web version of this article.)

organization of α-SMA visualized as long aligned fibers, whereas the other hydrogels displayed immature, less organized, and prominent punctured structures. Secondary antibody controls were included in the experiments to verify specific staining of α-SMA (Fig. S2). On the gene level, the fibroblasts seeded on Col gels had a significantly higher mRNA expression of α-SMA (*ACTA2*) ($P < 0.001$) compared to both LC gels and CD gels (Fig. 7a). Fibroblasts cultured on Col gels and LC gels showed a lower expression of collagen type 1 mRNA (*COL1A2*) compared to cells cultured on CD gels (Fig. 7b).

The mRNA expression of the *SDC4* gene in fibroblasts seeded on Col gels was significantly higher than the LC gels ($P < 0.001$) and higher, although not significant, than CD gels (Fig. 7c). The levels of SDC-4 shed by fibroblasts on the different collagen gels were variable, both within the same gel samples and between gel types, indicating a spontaneous shedding. The experiment was repeated with two different ELISA kits, with similar results. The levels of shed SDC-4 from fibroblasts seeded on LC gels were significantly higher than Col gels ($P \leq 0.05$), while the fibroblasts seeded on CD gels tended to be higher than Col gels with a similar average protein level as LC gels (Fig. 7d). The ratio between secreted MMP-2 and its inhibitor TIMP-2 is presented (Fig. 7e). The ratio can be used as an indication for the enzyme activity and was calculated based on the results from the ELISA experiments for MMP-2 and TIMP-2. The MMP-2/TIMP-2 ratio for the cells on LC gels was significantly higher than CD gels ($P \leq 0.01$) and higher, although not significant, than Col gels. The difference between the Col gels and CD gels was not significant. The MMP-2 and TIMP-2 raw data are included in the supplementary material (Fig. S3). The cells seeded on Col gels showed significantly higher MMP-2 protein secretion than the LC gels ($P \leq 0.05$). There was no significant difference in the MMP-2 protein secretion between LC gels and the gels made with HPβCD. The cells seeded on LC gels had the

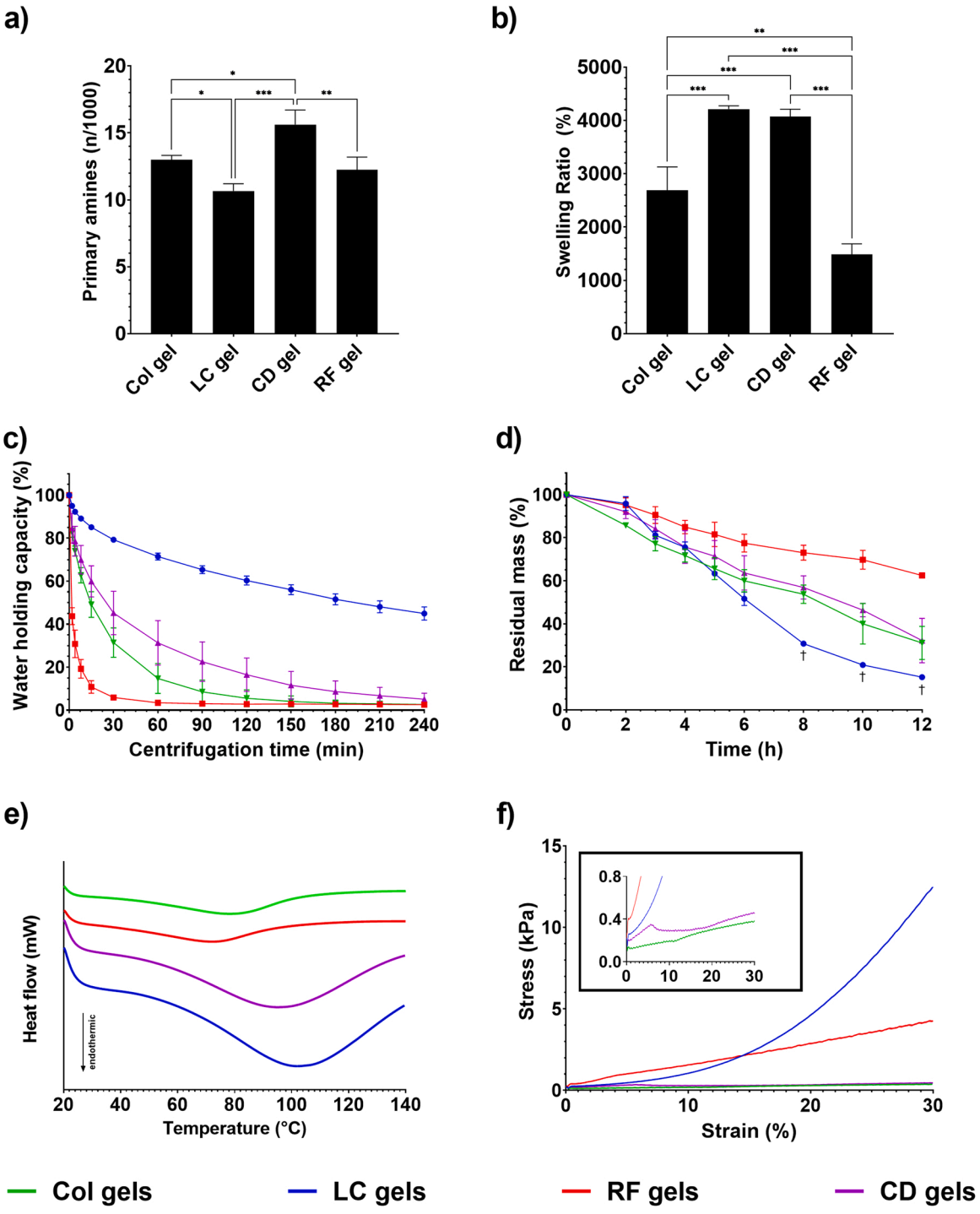


**Fig. 3.** Physical properties of hydrogels. a) Content of primary amines per 1000 amino acids (n/1000). LC gels exhibited the lowest content of primary amines, indicating the highest crosslinking of the collagen structure. b) Swelling ratio as % (w/w) of freeze-dried hydrogels. LC gels and CD gels appeared to have similar water absorption, while RF gels had the lowest swelling ability. c) Water holding capacity as % (w/w) of hydrogels subjected to 394*g* centrifugal force, with LC gels having a superior water holding capacity compared to Col gels, CD gels and RF gels, where the latter had the lowest capacity. d) Enzyme-mediated scaffold degradation by collagenase, showing highest resistance to collagenase for RF gels (points marked with a dagger (†) for LC gels had only one replicate due to low mechanical strength after collagenase digestion). e) Thermograms of freeze-dried collagen hydrogels illustrating the change in shrinkage temperature by crosslinking. LC and CD gels exhibited the highest shrinkage temperature, possibly due to CD complexation. f) Representative stress-strain curves of hydrogels between 0% and 30% strains. Col gels (green), LC gels (blue), RF gels (red), CD gels (purple). Asterisks (*) denote significant differences. Statistical analysis was performed by one way ANOVA with Tukey's multiple comparison test (* $P \leq 0.05$, ** $P \leq 0.01$, *** $P \leq 0.001$). (For interpretation of the references to color in this figure legend, the reader is referred to the web version of this article.)

**Table 3**
Results from macroindentation of collagen hydrogels.

| Gel sample | Young's modulus (20% strain) | Ultimate compressive strength | Fracture point |
|---|---|---|---|
| *Col gels* | 3.50 ± 0.21 kPa | ≥ 0.43 ± 0.04 kPa | ≥ 60% strain |
| *LC gels* | 62.30 ± 7.95 kPa | 16.05 ± 4.93 kPa | 25–35% strain |
| *RF gels* | 30.88 ± 0.51 kPa | ≥ 11.89 ± 0.49 kPa | ≥ 60% strain |
| *CD gels* | 3.90 ± 0.40 kPa | ≥ 0.57 ± 0.05 kPa | ≥ 60% strain |

lowest TIMP-2 protein secretion of all samples. There was no significant difference in the TIMP-2 secretion between Col gels and CD gels.

## 4. Discussion

In this study, we developed a hydrogel based on CD modulated collagen and LC photocrosslinking to tailor the properties of the material. CDs are known to interact with collagen by binding with hydrophobic amino acids in the protein chain. This has previously been shown to reduce the fibril diameter during gelation, and provide increased viscosity, mechanical strength and transparency [22]. The LC gels were clearly more transparent compared to Col gels and RF gels after completed photocrosslinking and incubation. The CD gels without LC did, however, become translucent, similar to the Col gels. A change in the crosslinking procedure from irradiation before to irradiation after incubation for 1 h (as used in the RF photocrosslinking procedure) resulted in more translucent gels but quite similar mechanical strength (data not shown). The ability of LC photocrosslinking to achieve gelling already after 10 s of irradiation may be crucible for the organization of collagen fibrils and transparency. This will further increase the potential for use in applications requiring immediate gelation. The difference in fibril formation and organization was confirmed by SEM imaging. The Col and CD gels were comparable with randomly organized fibrils within the hydrogel, while RF gels seemed to have a somewhat denser organization of the fibrils. The LC gels were, however, completely different from the other samples with indication of a denser collagen network throughout the hydrogel. Transparent materials are desirable for certain applications, like in the eye [43]. Based on these observations, and the ease of the crosslinking procedure, the further photocrosslinking irradiation was performed directly after neutralization and before the final incubation.

The swelling ratio, water holding capacity, content of primary amines, thermal properties, enzymatic resistance, and mechanical properties of the hydrogels depended on the crosslinking procedure. The RF gels exhibited a low swelling ratio and water holding capacity, despite a high Young's modulus and a high enzymatic resistance to collagenase. This indicates a higher crosslinking of the structure with a higher density of fibrils [44,45]. The reduction in primary amines in RF gels and LC gels compared to the other gels confirmed that the crosslinking reaction involved primary amine groups. Amine groups are known to participate in photocrosslinking reactions involving collagen and a photosensitizer, such as in corneal CXL treatment with RF and UVA, although to a minor extent [46]. The shrinkage temperature of collagen can usually be observed as a broad endothermic peak at around 80 °C [47]. The shrinkage temperature of RF gels was not significantly different from Col gels, indicating only a slightly higher crosslinking density. LC gels had the highest reduction in primary amines and the largest increase in shrinkage temperature compared to the non-crosslinked samples, indicating the most crosslinked hydrogel. Further, the water holding capacity of the LC gels was superior to the other hydrogels. This was probably due to denser network of the collagen by photocrosslinking before further physical crosslinking by incubation [22,48]. The potential influence on water absorption and thermostabilization by CD modulation was studied by comparing the properties of LC gels with CD gels prepared without LC and photocrosslinking. The swelling of LC gels and CD gels was similar, which may be due to the content of HPβCD in both gels. The similarity in shrinkage temperature indicated that the increased transition temperature after LC photocrosslinking may be ascribed to modulation by CDs, rather than a

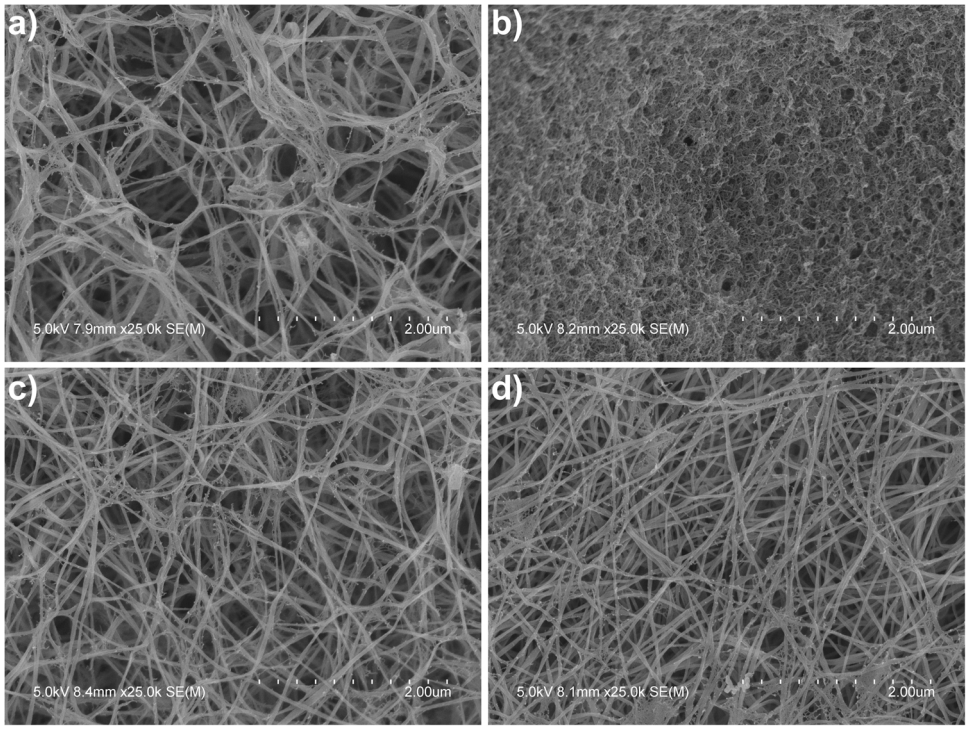


**Fig. 4.** Scanning Electron Microscopy (SEM) images showing the hydrogel microstructure. a) Col gels, b) LC gels, c) CD gels, d) RF gels. The microstructure of the LC gels differed from the other hydrogels by a denser collagen network, while the other hydrogels were composed of fibrillar structures. Scale bars: 2 μm.

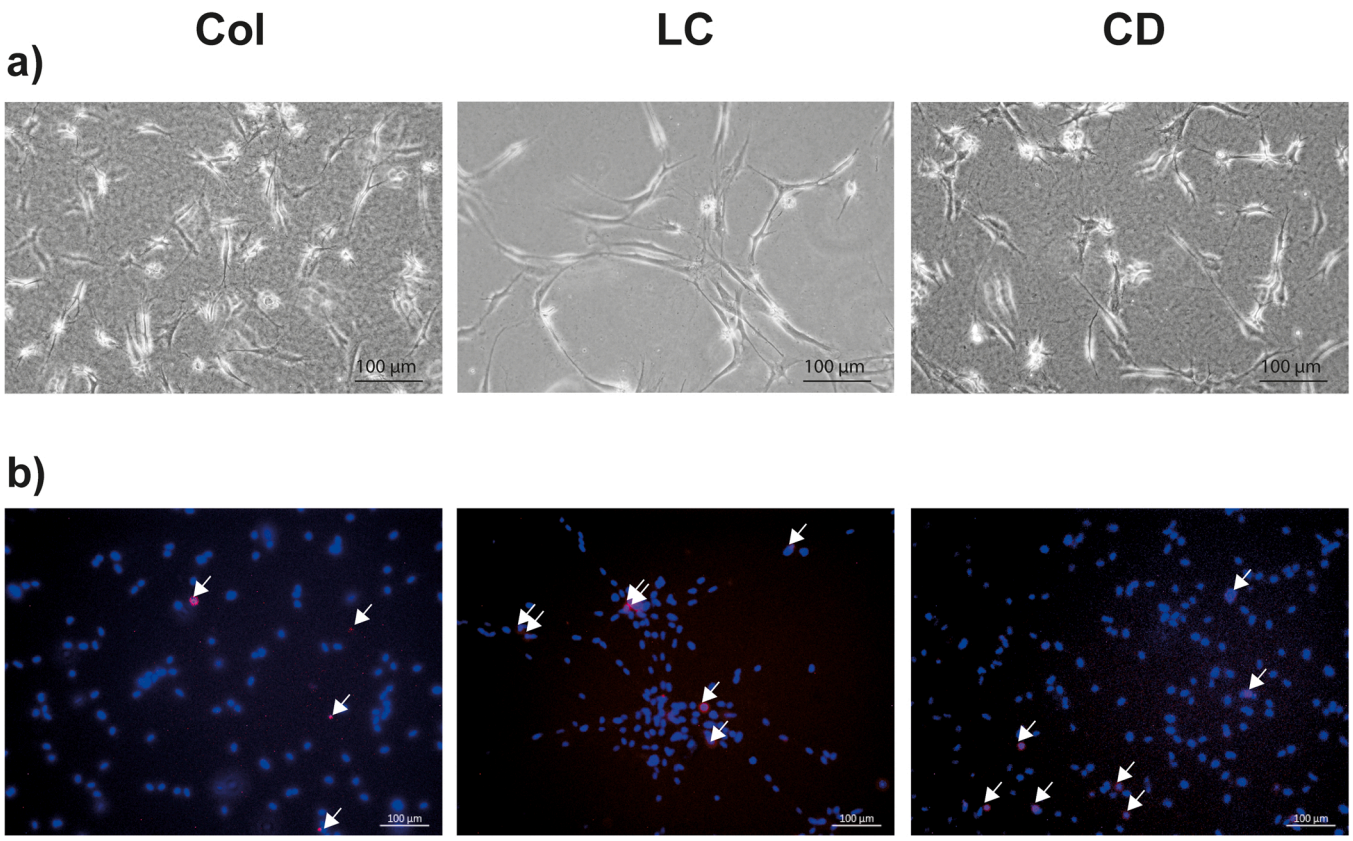


**Fig. 5.** Fibroblast morphology and viability on hydrogels. a) Light microscopy images of fibroblasts seeded on the hydrogels showing even dispersion of fibroblasts on Col gels and CD gels, while fibroblasts on LC gels seemed to cluster or collectively migrate through the gel. b) Staining of cell nuclei (blue) and dead cells (red, marked with arrows) mainly showing viable cells for fibroblasts seeded on Col gels, LC gels and CD gels. The images are representative for the whole sample area. (For interpretation of the references to color in this figure legend, the reader is referred to the web version of this article.)

higher crosslinking density. The LC gels were the least resistant to collagenase degradation. As suggested by other researchers, gelation by irradiation at low temperatures results in hydrogels with low fibril density and low resistance to enzymatic degradation [49]. In cases where there is an elevated level of MMPs, like collagenases, the LC gels may be broken down to smaller fragments in a shorter time than collagen hydrogels prepared by other crosslinking procedures. This indicates a good biodegradability. Further, the collagenase effect is dependent on the availability of the site of cleavage and may be influenced by the difference in fibril organization after crosslinking [50]. The water holding capacity is on the other hand a measurement of the hydrogen bonding ability and may be an indication of a change in crosslinking [51–53]. The difference in swelling ratio and water holding capacity between the gels corresponded to the variation in crosslinking of the structures and was supported by the difference in resistance to collagenase. The crosslinking will further change the mechanical strength [54]. This resulted in more brittle LC gels, but with a high Young's modulus (higher elasticity). The high elasticity, swelling ratio and water retention may be desirable in tissue engineering applications, as it will facilitate the diffusion and retention of nutrition and provide elasticity and flexibility similar to the native extracellular matrix and make the hydrogels less prone to collapse [49,55].

Fibroblasts were seeded on top of the produced gels. By examining the cell distribution, some of the cells seemed to migrate into the gels. Most of the cells were, however, still distributed on the gel surface after 48 h (results not shown). The 3D migration through the gels were not studied further. The cell viability was high on Col gels, LC gels and CD gels, illustrated by a higher number of live cell nuclei compared to the low number of dead cells. Interestingly, the RF gels did not facilitate cell growth. This is in contrast to other relevant studies using gels prepared with the same RF concentration and similar photocrosslinking procedure, in which the RF crosslinked scaffolds were used for fibrochondrocytes with excellent viability [56]. The only differences between the RF gels and the Col gels, were the addition of 0.01% (w/v) RF and a photocrosslinking procedure after 1 h incubation in the former. The gels were incubated for 30 min after irradiation to complete crosslinking, before addition of cells. A potential explanation is the formation of hydrogen peroxide ($H_2O_2$) during irradiation of RF in the presence of certain amino acids [57]. Measurements of peroxide content in the hydrogels after complete crosslinking procedure revealed that peroxides were present in RF gels while absent in the other gels, confirming peroxide-induced cytotoxicity for fibroblasts in RF gels. The toxicity of similar concentrations of $H_2O_2$ has been studied by others showing accelerated senescence and reduced viability in fibroblasts [58]. This suggested the need for a reduction in irradiation time during the preparation of collagen constructs. Based on these results, the RF gels were not included in the further cell studies.

The differentiation of fibroblasts into myofibroblasts on gels is known to be dependent on, among other factors, the gel rigidity [59]. The myofibroblasts play an important role in the wound healing process, promoting matrix synthesis and wound contraction [60]. Cells cultured on a rigid surface, like the bottom of a well plate or a rigid gel, can differentiate into myofibroblasts at low seeding densities [61,62]. The cells were seeded with similar density for all samples, and with a density more than 3-fold higher than the reported values in the literature (for RT-qPCR experiments). Further, the results indicated that the differentiation was a result of the material and not the seeding density. The LC gels exhibited remarkably higher stress at lower strains, which can influence the myofibroblast differentiation. Even though the mRNA expression of α-SMA by fibroblasts seeded on LC gels and CD gels was

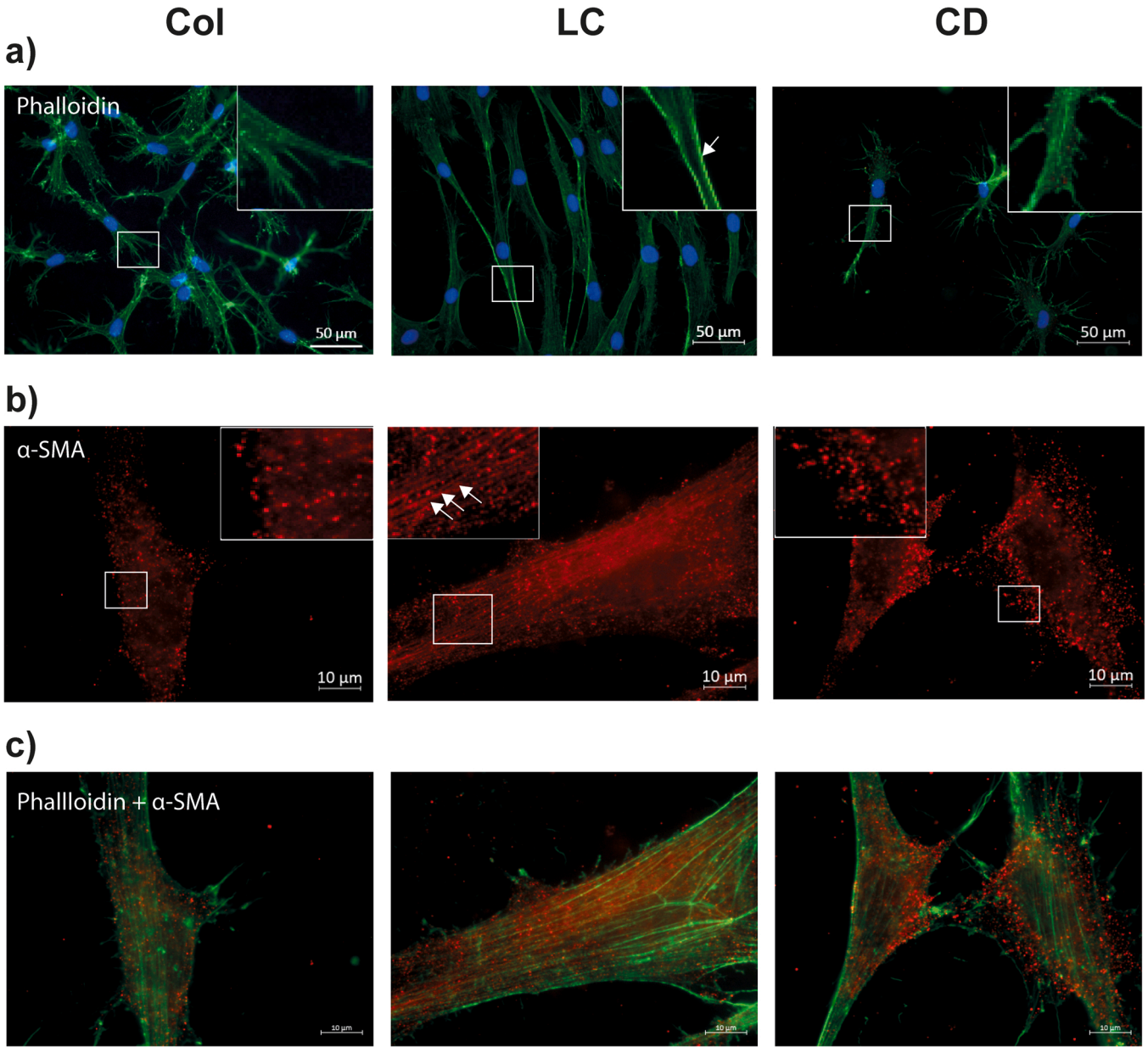


**Fig. 6.** Hydrogel crosslinking procedures influences fibroblast F-actin stress fibers and myofibroblast differentiation. a) Fluorescence microscopy of F-actin (phalloidin, green) and cell nuclei (blue), showing more prominent intracellular stress fibers in the Col and CD gels, while cells seeded onto LC gels had stronger staining of peripheral stress fibers. b) Immunostaining of α-SMA (red) showing organized smooth muscle actin fibers (marked by arrow heads) for LC gels rather than immature fibers as seen for Col and CD gels. c) Co-staining of F-actin (phalloidin, green) and α-SMA (red). (For interpretation of the references to color in this figure legend, the reader is referred to the web version of this article.)

somewhat low and the fibroblasts seeded on the Col gels expressed higher α-SMA expression at the time of sampling, the immunofluorescence results showed that the LC gels contained fibroblasts with more organized α-SMA. This may indicate that the onset of myofibroblast differentiation was earlier in fibroblasts grown on LC gels, reflecting the observed downregulation of α-SMA at mRNA level. This was further supported by the appearance of α-SMA in Col gels and CD gels, expressed as an unorganized grainy pattern, rather than fibers.

SDC-4 is a regulator of fibroblast cell adhesion and migration by regulating focal adhesion and actin-cytoskeletal organization formation in fibroblasts. SDC-4 shedding of its ectodomain results in an altered distribution of cytoskeletal components, functional loss of adhesion, and gain of migratory capacities [63]. Our results showed a redistribution of stress fibers in LC gels, which is a morphological characteristic observed in less adhesive and more migratory cells [64,65]. An increased SDC-4 shedding, although not significant, was observed from cells grown on LC gels. Together with less SDC-4 production and reorganized actin-cytoskeletal components of less adhesive cells, this could reflect SDC-4 receptor mechanisms to be involved in attachment, spreading and migratory behavior of the fibroblast influenced by LC gel structure. Interestingly, a smaller fibril size of electrospun polycaprolactone (PCL)-based fibers has shown to contribute to an increased adhesion, velocity, and migratory behavior of fibroblasts [66,67]. In the same study, smaller fibril size also upregulated the expression of α-SMA, the myofibroblast phenotype. This is in line with our data with fibroblasts of myofibroblast phenotype in the LC gels. We suggest heterogeneity of fibroblasts to be present on the LC gels, with some less adhesive and migratory together with more α-SMA expressing of myofibroblast phenotype.

MMP-2 is an enzyme involved in wound healing and remodeling of

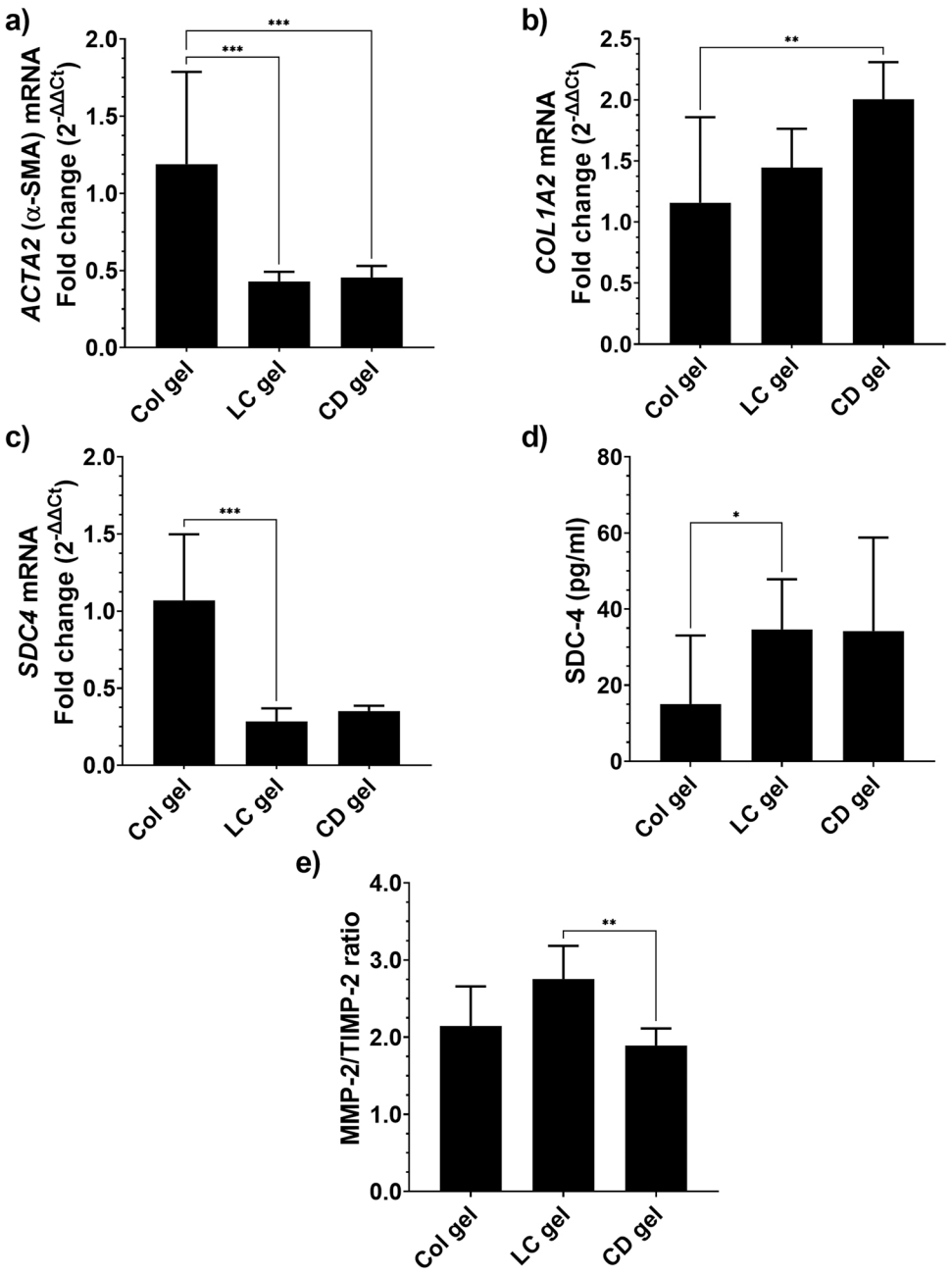


**Fig. 7.** mRNA expression and secretion of proteins related to fibroblast differentiation and MMP activity are changed upon crosslinking of the hydrogels. mRNA expression is presented as the relative and normalized mRNA (fold change) in cells seeded on hydrogels compared to cells seeded on Col gels. Protein secretion is presented as the average protein concentration. The hydrogel crosslinking procedure affects the expression of a) *ACTA2* (α-SMA) mRNA, b) *COL1A2* (collagen type I alpha 2 chain) mRNA, c) *SDC4* mRNA, d) SDC-4 shedding and e) MMP-2/TIMP-2 ratio calculated based on the secretion of protein into the cell media. The data was collected from three independent biological experiments, each with three technical replicates. Asterisks (*) denote significant differences. Statistical analysis was performed by one-way ANOVA with Tukey's multiple comparison test for normally distributed samples (*ACTA2* and *COL1A2*) and Kruskal-Wallis test with Dunn's multiple comparison for samples not following a normal distribution (*SDC4 mRNA*, SDC-4 shedding and MMP-2/TIMP-2 ratio) (* $P \leq 0.05$, ** $P \leq 0.01$, *** $P \leq 0.001$).

the extracellular matrix by promoting migration of fibroblasts to the wound site [68]. The ratio between the protein secretion of MMP-2 and its inhibitor, TIMP-2, indicated a balance of the expression of the proteins pointing towards MMP-2 for cells seeded on all of the gels. Fibroblasts seeded on LC gels had the highest MMP-2/TIMP-2 ratio. The MMP-2 and TIMP-2 levels were, however, lower in cells grown on the LC and CD gels, indicating a lower release or complexation of the enzyme. A possible explanation is complexation of MMPs with TIMPs or that the protein is shielded by complexation with CDs. The ratio of MMP-2/TIMP-2 was higher for cells seeded on LC compared to the other gels, suggesting that complexation with TIMPs may explain the lower enzyme levels.

The increased SDC-4 shedding from fibroblasts seeded on collagen hydrogels can potentially be due to an elevated MMP-2/TIMP-2 ratio, whereas MMP-2 is known to cleave SDC-4 [69]. In addition, other enzymes, such as ADAMS (disintegrin and metalloprotease) and serine proteases not investigated in our study, can also be involved in SDC-4 shedding mechanisms [70,71]. The *COL1A2* mRNA expression for fibroblasts seeded on CD gels was significantly higher than Col gels. LC gels also tended to have a higher expression of *COL1A2* than Col gels (although not significant). The levels of TIMP-2 were highest in Col gels, which can explain the somewhat lower *COL1A2* mRNA expression for the same gels, whereas the addition of TIMP-2 has shown to suppress collagen synthesis and mRNA expression in keloid fibroblasts [72]. In wild-type cardiac fibroblasts, myofibroblast differentiation was associated with increased α-SMA and collagen mRNA expression. However, a knockout of SDC-4 decreased these. [73]. We did not obtain this clear correlation at mRNA level, which could reflect heterogeneity in our fibroblast phenotypes, or also difference in comparing SDC-4 knockout cells with SDC-4 expressing cells. In our study, the fibroblasts expressed SDC-4.

The mechanisms of RF photocrosslinking of collagen have previously been discussed and thoroughly studied [74]. LC photocrosslinking of collagen to a firm gel can as demonstrated in the present work, be

performed at 4 °C without further crosslinking. Photocrosslinking with RF needs to be performed after incubation at 37 °C to form a firm gel [14, 56, 75]. RF is rapidly photodecomposed to LC within minutes under certain experimental conditions [17]. This might indicate that the photocrosslinking by RF actually is a result of the photochemical degradation of the photosensitizer. This hypothesis is further supported by studies on the phototoxic effect of RF, being a hydrophilic substance, while LC is lipophilic and can penetrate the bacterial membrane [18]. Further, the crosslinking effect can be due to the formation of ROS and singlet oxygen ($^1O_2$) by excitation of RF, supported by the ability of quenchers to inhibit the photocrosslinking properties of RF [75,76]. Similar mechanisms can occur in the presence of LC. The quantum yield of $^1O_2$ formation by LC at 365 nm exposure is more than 30% higher than for RF in aqueous media ($\Phi_{RF} = 0.48$, $\Phi_{LC} = 0.63$) [17].

In addition to good mechanical properties and excellent water holding capacity, it is important that scaffolds for tissue engineering, e.g., eye applications and in wound treatment allow for sufficient exchange of nutrients and oxygen. The fibroblasts in the present work were seeded on top of the hydrogels. The translation of the present results (in 2D) to the proposed applications (in 3D) can, however, be challenging. The LC photocrosslinked scaffolds are currently further developed in our lab and will therefore be assessed for their suitability in tissue engineering (3D cultures) and wound healing in future work.

## 5. Conclusions

This study has demonstrated the effects of LC photocrosslinking of collagen hydrogels. This photocrosslinking method reduced the gelation time to 10 s prior to optional physical crosslinking. The gels exhibited stronger water holding capacity, higher elasticity and thermal stability and the highest crosslinking density compared to Col gels and RF gels. The use of CDs in the hydrogel formulation increased the solubility of LC and potentially contributed to increased transparency, high thermostability and good physical properties of the hydrogel. Cell studies on human fibroblasts cultured in 2D indicated good biocompatibility and a suggested migratory behavior when seeded on the LC gel. Further, the fibroblasts seemed to differentiate into myofibroblasts. LC is an endogenous compound and LC photocrosslinking of collagen offers an alternative to other potentially toxic crosslinkers. Further studies of fibroblast behavior in 3D and in vivo have to be performed to assess the suitability in tissue engineering and wound healing.

## Funding

This work was partially supported by a grant from Norwegian Fund for Research Fees for Agricultural Products ("SusHealth", no. 314599) and Norilia AS (Oslo, Norway). The funders had no role in study design, data collection and analysis, decision to publish, or preparation of the manuscript.

## CRediT authorship contribution statement

**K. G. Grønlien:** Conceptualization, Investigation, Visualization, Writing – original draft, Writing – review & editing. **M. E. Pedersen:** Conceptualization, Supervision, Investigation, Writing – original draft, Writing – review & editing. **S. B. Rønning:** Supervision, Investigation, Visualization, Writing – original draft, Writing – review & editing. **N. T. Solberg:** Supervision, Investigation, Writing – review & editing. **H. H. Tønnesen:** Conceptualization, Funding acquisition, Supervision, Writing – original draft, Writing – review & editing.

## Declaration of Competing Interest

The authors declare that they have no known competing financial interests or personal relationships that could have appeared to influence the work reported in this paper.

## Acknowledgments

The authors are grateful to Bente Amalie Breiby, Department of Pharmacy, University of Oslo, Ulrike Böcker, Silje Kristine Bergum, R. Christel Andreassen and Kenneth Aase Kristoffersen, Nofima AS for technical support, Karen Wahlstrøm Sanden, Nofima AS for isolation of collagen from turkey tendon and Raj Kumar Thapa, Department of Pharmacy, University of Oslo, for valuable discussions. SEM images were acquired by Antje Hofgaard, Department of Biosciences, University of Oslo. Turkey tendon by-products and financial support for isolation of collagen from turkey were contributed by Norilia AS.

## Appendix A. Supporting information

Supplementary data associated with this article can be found in the online version at doi:10.1016/j.mtcomm.2022.103635.

## References

[1] M.D. Shoulders, R.T. Raines, Collagen structure and stability, Annu. Rev. Biochem. 78 (2009) 929–958.
[2] C. Frantz, K.M. Stewart, V.M. Weaver, The extracellular matrix at a glance, J. Cell Sci 123 (24) (2010) 4195–4200.
[3] W. Aljohani, M.W. Ullah, X. Zhang, G. Yang, Bioprinting and its applications in tissue engineering and regenerative medicine, Int. J. Biol. Macromol. 107 (2018) 261–275.
[4] P. Abdollahiyan, B. Baradaran, M. de la Guardia, F. Oroojalian, A. Mokhtarzadeh, Cutting-edge progress and challenges in stimuli responsive hydrogel microenvironment for success in tissue engineering today, J. Control Release 328 (2020) 514–531.
[5] X. Cui, J. Li, Y. Hartanto, M. Durham, J. Tang, H. Zhang, G. Hooper, K. Lim, T. Woodfield, Advances in extrusion 3D bioprinting: a focus on multicomponent hydrogel-based bioinks, Adv. Healthc. Mater. 9 (15) (2020), 1901648.
[6] J.A. Hunt, R. Chen, T. van Veen, N. Bryan, Hydrogels for tissue engineering and regenerative medicine, J. Mater. Chem. B 2 (33) (2014) 5319–5338.
[7] J.L. Drury, D.J. Mooney, Hydrogels for tissue engineering: scaffold design variables and applications, Biomaterials 24 (24) (2003) 4337–4351.
[8] A. De Mori, M. Peña Fernández, G. Blunn, G. Tozzi, M. Roldo, 3D printing and electrospinning of composite hydrogels for cartilage and bone tissue engineering, Polymers 10 (3) (2018) 285.
[9] T.J. Hinton, Q. Jallerat, R.N. Palchesko, J.H. Park, M.S. Grodzicki, H.-J. Shue, M. H. Ramadan, A.R. Hudson, A.W. Feinberg, Three-dimensional printing of complex biological structures by freeform reversible embedding of suspended hydrogels, Sci. Adv. 1 (9) (2015), e1500758.
[10] N. Ashammakhi, S. Ahadian, C. Xu, H. Montazerian, H. Ko, R. Nasiri, N. Barros, A. Khademhosseini, Bioinks and bioprinting technologies to make heterogeneous and biomimetic tissue constructs, Mater. Today Bio 1 (2019), 100008.
[11] J. Gopinathan, I. Noh, Recent trends in bioinks for 3D printing, Biomater Res. 22 (2018), 11-11.
[12] E.O. Osidak, P.A. Karalkin, M.S. Osidak, V.A. Parfenov, D.E. Sivogrivov, F.D.A. S. Pereira, A.A. Gryadunova, E.V. Koudan, Y.D. Khesuani, V.A. Kasyanov, S. I. Belousov, S.V. Krasheninnikov, T.E. Grigoriev, S.N. Chvalun, E.A. Bulanova, V. A. Mironov, S.P. Domogatsky, Viscoll collagen solution as a novel bioink for direct 3D bioprinting, J. Mater. Sci. Mater. Med. 30 (3) (2019) 31.
[13] G. Tronci, C.A. Grant, N.H. Thomson, S.J. Russell, D.J. Wood, Multi-scale mechanical characterization of highly swollen photo-activated collagen hydrogels, J. R. Soc. Interface 12 (102) (2015), 20141079.
[14] N. Diamantides, L. Wang, T. Pruiksma, J. Siemiatkoski, C. Dugopolski, S. Shortkroff, S. Kennedy, L.J. Bonassar, Correlating rheological properties and printability of collagen bioinks: the effects of riboflavin photocrosslinking and pH, Biofabrication 9 (3) (2017), 034102.
[15] G. Wollensak, E. Spoerl, T. Seiler, Riboflavin/ultraviolet-a–induced collagen crosslinking for the treatment of keratoconus, Am. J. Ophthalmol. 135 (5) (2003) 620–627.
[16] R. Huang, H.J. Kim, D.B. Min, Photosensitizing effect of riboflavin, lumiflavin, and lumichrome on the generation of volatiles in soy milk, J. Agric. Food Chem. 54 (6) (2006) 2359–2364.
[17] C.K. Remucal, K. McNeill, Photosensitized amino acid degradation in the presence of riboflavin and its derivatives, Environ. Sci. Technol. 45 (12) (2011) 5230–5237.
[18] V.J.V. Bergh, E. Bruzell, A.B. Hegge, H.H. Tønnesen, Influence of formulation on photoinactivation of bacteria by lumichrome, Pharmazie 70 (9) (2015) 574–580.
[19] S.V. Kurkov, T. Loftsson, Cyclodextrins, Int. J. Pharm. 453 (1) (2013) 167–180.
[20] A. Hedges, Chapter 22 - Cyclodextrins: Properties and Applications, in: J. BeMiller, R. Whistler (Eds.), Starch, Third edition.,, Academic Press, San Diego, 2009, pp. 833–851.
[21] R. Vaitkus, G. Grinciene, E. Norkus, Peculiarities of β-cyclodextrin acid hydrolysis, Chemija 19 (2008).
[22] S. Majumdar, X. Wang, S.D. Sommerfeld, J.J. Chae, E.-N. Athanasopoulou, L. S. Shores, X. Duan, L.M. Amzel, F. Stellacci, O. Schein, Q. Guo, A. Singh, J.

H. Elisseeff, Cyclodextrin modulated type I collagen self-assembly to engineer biomimetic cornea implants, Adv. Funct. Mater. 28 (41) (2018), 1804076.
[23] W.K. Grier, A.S. Tiffany, M.D. Ramsey, B.A.C. Harley, Incorporating β-cyclodextrin into collagen scaffolds to sequester growth factors and modulate mesenchymal stem cell activity, Acta Biomater. 76 (2018) 116–125.
[24] Y. Chen, W. Song, X. Zhao, Q. Han, L. Ren, An antibacterial collagen membrane crosslinked by the inclusion complex of β-cyclodextrin dialdehyde and ofloxacin for bacterial keratitis, RSC Adv 8 (32) (2018) 18153–18162.
[25] A.E. Postlethwaite, J.M. Seyer, A.H. Kang, Chemotactic attraction of human fibroblasts to type I, II, and III collagens and collagen-derived peptides, Proc. Natl. Acad. Sci. USA 75 (2) (1978) 871–875.
[26] S. Chattopadhyay, R.T. Raines, Collagen-based biomaterials for wound healing, Biopolymers 101 (8) (2014) 821–833.
[27] B. Hinz, The role of myofibroblasts in wound healing, Curr. Res. Transl. Med. 64 (4) (2016) 171–177.
[28] B. Hinz, G. Gabbiani, Cell-matrix and cell-cell contacts of myofibroblasts: role in connective tissue remodeling, Thromb. Haemost. 90 (12) (2003) 993–1002.
[29] M.P. Caley, V.L.C. Martins, E.A. O'Toole, Metalloproteinases and wound healing, Adv. Wound Care 4 (4) (2015) 225–234.
[30] T. Manon-Jensen, Y. Itoh, J.R. Couchman, Proteoglycans in health and disease: the multiple roles of syndecan shedding, FEBS J 277 (19) (2010) 3876–3889.
[31] R. Brooks, R.C. Williamson, M.D. Bass, Syndecan-4 independently regulates multiple small GTPases to promote fibroblast migration during wound healing, Small GTPases 3 (2) (2012) 73–79.
[32] S. Gopal, A. Bober, J.R. Whiteford, H.A. Multhaupt, A. Yoneda, J.R. Couchman, Heparan sulfate chain valency controls syndecan-4 function in cell adhesion, J. Biol. Chem. 285 (19) (2010) 14247–14258.
[33] S. Gopal, H.A.B. Multhaupt, R. Pocock, J.R. Couchman, Cell-extracellular matrix and cell-cell adhesion are linked by syndecan-4, Matrix Biol 60–61 (2017) 57–69.
[34] T.T. Vuong, T.M. Reine, A. Sudworth, T.G. Jenssen, S.O. Kolset, Syndecan-4 Is a major syndecan in primary human endothelial cells in vitro, modulated by inflammatory stimuli and involved in wound healing, J. Histochem. Cytochem. 63 (4) (2015) 280–292.
[35] K.G. Grønlien, M.E. Pedersen, K.W. Sanden, V. Høst, J. Karlsen, H.H. Tønnesen, Collagen from turkey (Meleagris gallopavo) tendon: a promising sustainable biomaterial for pharmaceutical use, Sustain. Chem. Pharm. 13 (2019), 100166.
[36] R. Mao, J. Tang, B.G. Swanson, Water holding capacity and microstructure of gellan gels, Carbohydr. Polym. 46 (4) (2001) 365–371.
[37] D. Lee, H. Zhang, S. Ryu, Elastic Modulus Measurement of Hydrogels, in: M.I. H. Mondal (Ed.), Cellulose-Based Superabsorbent Hydrogels, Springer International Publishing, Cham, 2018, pp. 1–21.
[38] N. Davidenko, C.F. Schuster, D.V. Bax, N. Raynal, R.W. Farndale, S.M. Best, R. E. Cameron, Control of crosslinking for tailoring collagen-based scaffolds stability and mechanics, Acta Biomaterialia 25 (2015) 131–142.
[39] S.G. Wubshet, D. Lindberg, E. Veiseth-Kent, K.A. Kristoffersen, U. Böcker, K. E. Washburn, N.K. Afseth, Chapter 8 - Bioanalytical Aspects in Enzymatic Protein Hydrolysis of By-Products, in: C.M. Galanakis (Ed.), Proteins: Sustainable Source, Processing and Applications, Academic Press, 2019, pp. 225–258.
[40] R.J. Whitehurst, B.A. Law, Enzymes in Food Technology, Sheffield Academic Press, 2002.
[41] S.A. Bustin, J.-F. Beaulieu, J. Huggett, R. Jaggi, F.S.B. Kibenge, P.A. Olsvik, L. C. Penning, S. Toegel, MIQE précis: practical implementation of minimum standard guidelines for fluorescence-based quantitative real-time PCR experiments, BMC Mol. Biol. 11 (1) (2010) 74.
[42] T.D. Schmittgen, K.J. Livak, Analyzing real-time PCR data by the comparative CT method, Nat. Protoc. 3 (6) (2008) 1101–1108.
[43] G.M. Fernandes-Cunha, K.M. Chen, F. Chen, P. Le, J.H. Han, L.A. Mahajan, H. J. Lee, K.S. Na, D. Myung, In situ-forming collagen hydrogel crosslinked via multi-functional PEG as a matrix therapy for corneal defects, Sci. Rep. 10 (1) (2020) 16671.
[44] C. Yang, Enhanced physicochemical properties of collagen by using EDC/NHS-crosslinking, Bull. Mater. Sci. 35 (5) (2012) 913–918.
[45] V. Charulatha, A. Rajaram, Influence of different crosslinking treatments on the physical properties of collagen membranes, Biomaterials 24 (5) (2003) 759–767.
[46] A.S. McCall, S. Kraft, H.F. Edelhauser, G.W. Kidder, R.R. Lundquist, H.E. Bradshaw, Z. Dedeic, M.J.C. Dionne, E.M. Clement, G.W. Conrad, Mechanisms of corneal tissue cross-linking in response to treatment with topical riboflavin and long-wavelength ultraviolet radiation (UVA), Investig. Ophthalmol. Vis. Sci. 51 (1) (2010) 129–138.
[47] Y. Huang, Y. Wang, L. Chen, L. Zhang, Facile construction of mechanically tough collagen fibers reinforced by chitin nanofibers as cell alignment templates, J. Mater. Chem. B. 6 (6) (2018) 918–929.
[48] S. Hayes, P. Lewis, M.M. Islam, J. Doutch, T. Sorensen, T. White, M. Griffith, K. M. Meek, The structural and optical properties of type III human collagen biosynthetic corneal substitutes, Acta Biomater 25 (2015) 121–130.
[49] C. Xu, X. Wei, F. Shu, X. Li, W. Wang, P. Li, Y. Li, S. Li, J. Zhang, H. Wang, Induction of fiber-like aggregation and gelation of collagen by ultraviolet irradiation at low temperature, Int. J. Biol. Macromol. 153 (2020) 232–239.
[50] S. Perumal, O. Antipova, J.P.R.O. Orgel, Collagen fibril architecture, domain organization, and triple-helical conformation govern its proteolysis, Proc. Natl. Acad. Sci. USA 105 (8) (2008) 2824–2829.
[51] V.M. Gun'ko, I.N. Savina, S.V. Mikhalovsky, Properties of Water Bound in Hydrogels, Gels 3 (4) (2017).
[52] S. Mani, F. Khabaz, R.V. Godbole, R.C. Hedden, R. Khare, Structure and hydrogen bonding of water in polyacrylate gels: effects of polymer hydrophilicity and water concentration, J. Phys. Chem. B 119 (49) (2015) 15381–15393.
[53] K. Nam, T. Kimura, A. Kishida, Physical and biological properties of collagen-phospholipid polymer hybrid gels, Biomaterials 28 (20) (2007) 3153–3162.
[54] S. Lin, L. Gu, Influence of crosslink density and stiffness on mechanical properties of type I collagen gel, Materials 8 (2) (2015) 551–560.
[55] S. Mantha, S. Pillai, P. Khayambashi, A. Upadhyay, Y. Zhang, O. Tao, H.M. Pham, S.D. Tran, Smart hydrogels in tissue engineering and regenerative medicine, Materials 12 (20) (2019) 3323.
[56] J. Heo, R. Koh, W. Shim, H. Kim, H.-G. Yim, N. Hwang, Riboflavin-induced photo-crosslinking of collagen hydrogel and its application in meniscus tissue engineering, J. Control Release 6 (2) (2016) 148–158.
[57] S. Yoshimoto, N. Kohara, N. Sato, H. Ando, M. Ichihashi, Riboflavin plays a pivotal role in the UVA-induced cytotoxicity of fibroblasts as a key molecule in the production of H(2)O(2) by UVA radiation in collaboration with amino acids and vitamins, Int. J. Mol. Sci. 21 (2) (2020).
[58] J.-J. Lee, S.-C. Ng, J.-Y. Hsu, H. Liu, C.-J. Chen, C.-Y. Huang, W.-W. Kuo, Galangin reverses H2O2-induced dermal fibroblast senescence via SIRT1-PGC-1α/Nrf2 signaling, Int. J. Mol. Sci. 23 (3) (2022) 1387.
[59] E.E. Charrier, K. Pogoda, R.G. Wells, P.A. Janmey, Control of cell morphology and differentiation by substrates with independently tunable elasticity and viscous dissipation, Nat. Commun. 9 (1) (2018) 449.
[60] U.H. Ko, J. Choi, J. Choung, S. Moon, J.H. Shin, Physicochemically tuned myofibroblasts for wound healing strategy, Sci. Reports 9 (1) (2019) 16070.
[61] S.K. Masur, H.S. Dewal, T.T. Dinh, I. Erenburg, S. Petridou, Myofibroblasts differentiate from fibroblasts when plated at low density, Proc. Natl. Acad. Sci. U. S. A 93 (9) (1996) 4219–4223.
[62] A.M. Ruiz-Zapata, A. Heinz, M.H. Kerkhof, C. van de Westerlo-van Rijt, C.E. H. Schmelzer, R. Stoop, K.B. Kluivers, E. Oosterwijk, Extracellular matrix stiffness and composition regulate the myofibroblast differentiation of vaginal fibroblasts, Int. J. Mol. Sci. 21 (13) (2020) 4762.
[63] J.C. Rodríguez-Manzaneque, D. Carpizo, C. Plaza-Calonge Mdel, A.X. Torres-Collado, S.N. Thai, M. Simons, A. Horowitz, M.L. Iruela-Arispe, Cleavage of syndecan-4 by ADAMTS1 provokes defects in adhesion, Int. J. Biochem. Cell Biol. 41 (4) (2009) 800–810.
[64] P.S. Acharya, S. Majumdar, M. Jacob, J. Hayden, P. Mrass, W. Weninger, R. K. Assoian, E. Puré, Fibroblast migration is mediated by CD44-dependent TGF beta activation, J. Cell Sci 121 (Pt 9) (2008) 1393–1402.
[65] J.L. Rodríguez Fernández, B. Geiger, D. Salomon, A. Ben-Ze'ev, Suppression of vinculin expression by antisense transfection confers changes in cell morphology, motility, and anchorage-dependent growth of 3T3 cells, J. Cell Biol 122 (6) (1993) 1285–1294.
[66] S.R. Caliari, J.A. Burdick, A practical guide to hydrogels for cell culture, Nat. Methods 13 (5) (2016) 405–414.
[67] Y. Li, Z. Xiao, Y. Zhou, S. Zheng, Y. An, W. Huang, H. He, Y. Yang, S. Li, Y. Chen, J. Xiao, J. Wu, Controlling the multiscale network structure of fibers to stimulate wound matrix rebuilding by fibroblast differentiation, ACS Appl. Mater. Interfaces 11 (31) (2019) 28377–28386.
[68] E. Olaso, J.P. Labrador, L. Wang, K. Ikeda, F.J. Eng, R. Klein, D.H. Lovett, H.C. Lin, S.L. Friedman, Discoidin domain receptor 2 regulates fibroblast proliferation and migration through the extracellular matrix in association with transcriptional activation of matrix metalloproteinase-2, J. Biol. Chem. 277 (5) (2002) 3606–3613.
[69] T. Manon-Jensen, H.A. Multhaupt, J.R. Couchman, Mapping of matrix metalloproteinase cleavage sites on syndecan-1 and syndecan-4 ectodomains, FEBS J 280 (10) (2013) 2320–2331.
[70] D.R. Edwards, M.M. Handsley, C.J. Pennington, The ADAM metalloproteinases, Mol. Aspects Med. 29 (5) (2008) 258–289.
[71] A. Schmidt, F. Echtermeyer, A. Alozie, K. Brands, E. Buddecke, Plasmin- and thrombin-accelerated shedding of syndecan-4 ectodomain generates cleavage sites at Lys114–Arg115 and Lys129–Val130 bonds, Int. J. Biol. Chem 280 (41) (2005) 34441–34446.
[72] T. Dohi, K. Miyake, M. Aoki, R. Ogawa, S. Akaishi, T. Shimada, T. Okada, H. Hyakusoku, Tissue inhibitor of metalloproteinase-2 suppresses collagen synthesis in cultured keloid fibroblasts, Plast Reconstr. Surg. Glob. Open 3 (9) (2015) e520-e520.
[73] K.M. Herum, I.G. Lunde, B. Skrbic, G. Florholmen, D. Behmen, I. Sjaastad, C. R. Carlson, M.F. Gomez, G. Christensen, Syndecan-4 signaling via NFAT regulates extracellular matrix production and cardiac myofibroblast differentiation in response to mechanical stress, J. Mol. Cell Cardiol. 54 (2013) 73–81.
[74] L.A. Hapach, J.A. VanderBurgh, J.P. Miller, C.A. Reinhart-King, Manipulation of in vitro collagen matrix architecture for scaffolds of improved physiological relevance, Phys. Biol. 12 (6) (2015), 061002.
[75] A. Tirella, T. Liberto, A. Ahluwalia, Riboflavin and collagen: New crosslinking methods to tailor the stiffness of hydrogels, Mater. Lett. 74 (2012) 58–61.
[76] S. Sel, N. Nass, S. Pötzsch, S. Trau, A. Simm, T. Kalinski, G.I. Duncker, F.E. Kruse, G.U. Auffarth, H.J. Brömme, UVA irradiation of riboflavin generates oxygen-dependent hydroxyl radicals, Redox Rep. 19 (2) (2014) 72–79.
[77] T.B. McKay, S. Priyadarsini, D. Karamichos, Mechanisms of collagen crosslinking in diabetes and keratoconus, Cells 8 (10) (2019) 1239.